

Article

Optimal Vehicle Scheduling and Charging Infrastructure Planning for Autonomous Modular Transit System

Ande Chang ^{1,*}, Yuan Cong ², Chunguang Wang ^{3,*}  and Yiming Bie ² ¹ College of Forensic Sciences, Criminal Investigation Police University of China, Shenyang 110035, China² School of Transportation, Jilin University, Changchun 130022, China; congyuan128@126.com (Y.C.); yimingbie@126.com (Y.B.)³ State Key Laboratory for Strength and Vibration of Mechanical Structures, School of Aerospace Engineering, Xi'an Jiaotong University, Xi'an 710049, China

* Correspondence: changande@cipuc.edu.cn (A.C.); wangchunguang@xjtu.edu.cn (C.W.)

Abstract: Prioritizing the development of public transport is an effective way to improve the sustainability of the transport system. In recent years, bus passenger flow has been declining in many cities. How to reform the operating mode of the public transportation system is an important issue that needs to be solved. An autonomous modular bus (AMB) is capable of physical coupling and uncoupling to flexibly adjust vehicle capacity as well as provide high-quality service under unbalanced passenger demand conditions. To promote AMB adoption and reduce the operating cost of the bus route, this paper presents a joint optimization method to simultaneously determine the AMB dispatching plan, charging plan, and charging infrastructure configuration scheme. Then, a mixed-integer programming model is formulated to minimize the operating costs of the bus route. A hybrid intelligent algorithm combining enumeration, cloning algorithm, and particle swarm optimization algorithm is designed to resolve the formulated model. Subsequently, an actual bus route is taken as an example to validate the proposed method. Results indicate that the developed method in this paper can reduce the operating costs and operational energy consumption of the route compared with the real route operating plan. Specifically, the reduction ratio of the former is 23.85%, and the reduction ratio of the latter is 5.92%. The results of this study validate the feasibility and advantages of autonomous modular transit service, contributing positively to the sustainable development of the urban public transportation system.



Citation: Chang, A.; Cong, Y.; Wang, C.; Bie, Y. Optimal Vehicle Scheduling and Charging Infrastructure Planning for Autonomous Modular Transit System. *Sustainability* **2024**, *16*, 3316. <https://doi.org/10.3390/su16083316>

Academic Editor: Antonio Comi

Received: 24 January 2024

Revised: 21 March 2024

Accepted: 9 April 2024

Published: 16 April 2024



Copyright: © 2024 by the authors. Licensee MDPI, Basel, Switzerland. This article is an open access article distributed under the terms and conditions of the Creative Commons Attribution (CC BY) license (<https://creativecommons.org/licenses/by/4.0/>).

Keywords: autonomous modular bus; vehicle scheduling; charging infrastructure configuration; collaborative optimization; public transportation sustainability

1. Introduction

Prioritizing the promotion of public transportation is a proven way to reduce emissions from transport and improve the sustainability of society [1,2]. Recently, bus passenger flow has continued to decline in many cities. How to reform the operating mode of the public transportation system to improve the travel efficiency of passengers and reduce the operating costs of bus companies has become a vital issue for the current public transportation system. Nowadays, an emerging approach to urban public transportation, autonomous modular buses (AMBs), has attracted much attention [3,4]. The AMBs are electrically powered buses equipped with autonomous driving capabilities, which can operate independently on a specific route and physically couple and uncouple as operationally needed. This means that the spatiotemporal heterogeneity of passenger demand can be solved by adjusting the number of AMBs performing different trips [5–7]. Furthermore, it is permissible to specify which vehicle provides energy during the trip when several AMBs are coupled to perform a trip together. Generally, only the first vehicle of the coupled AMBs provides energy, and no energy is consumed by other vehicles. In such a case, when the first AMB has insufficient electricity, a group of AMBs can continue to perform a trip

by replacing the first AMB with the other one of the residual AMBs. During operation, the AMB with insufficient electricity can also return to the charging station for recharging individually. To sum up, AMBs can provide higher quality transit services at lower energy consumption and operating costs by adjusting vehicle capacity to change their service supply. The adoption of AMBs will significantly decrease environmental pollution, thus promoting the realization of a sustainable urban public transportation system.

From the above description, it is clear that the AMB dispatching problem not only involves assigning the trips in the timetable to the vehicles, but also arranging the order of AMBs that perform the same trip. Therefore, the dispatching methods for conventional fuel buses and electric buses are not suitable to be implemented in AMBs. The formulation for the AMB dispatching plan and charging plan is more complicated. On the one hand, due to the size constraints, the battery capacity of the AMB is limited and the battery needs to be recharged frequently during the daytime. On the other hand, which vehicle provides energy during the trip determines the state of charge (SOC) of each vehicle when several AMBs are connected together, and subsequently affects the AMB dispatching plan and charging plan. In addition, charging infrastructure configuration schemes also interact with the AMB dispatching plan and charging plan. Considering any of these problems individually may result in a sub-optimal transit system operating scheme [8]. Therefore, the integrated optimization of the AMB dispatching plan, charging plan, and charging infrastructure configuration plan is of great significance for a better transit system operation, and achieves the goals of reducing the operation costs of the modular transit network system (MTNS) and improving the theory of MTNS operation planning.

Hence, this study presents a collaborative optimization method to determine the AMB dispatching plan, charging plan, and charging infrastructure configuration plan. The main contributions of this study are as follows: (i) The SOC of the AMB is quantified under the condition that the first vehicle of the coupled AMBs provides energy during the entire trip. (ii) Considering the time-of-use tariff, we establish a nonlinear mixed-integer programming model that minimizes the operating costs. (iii) We use a combination of enumeration, cloning algorithm (CA), and particle swarm optimization (PSO) for designing a hybrid intelligent algorithm to solve the model and determine the AMB dispatching plan, charging plan, battery capacity, AMB fleet size, and number of chargers.

The structure of the paper is as follows: Section 2 reviews related literature discussing the integrated optimization of vehicle dispatching and charging infrastructure configuration and flexible capacity design for transit services. Section 3 describes the establishment process for the cooperative optimization model of AMB dispatching, charging scheduling, and charging infrastructure configuration and solution algorithm. Section 4 provides a case study on the basis of an actual bus route. Section 5 illustrates the research conclusions.

2. Literature Review

This study concentrates on the integrated optimization of vehicle dispatching and charging infrastructure configuration for the bus route operating AMB. Therefore, this paper discusses related work in terms of integrated optimization of vehicle dispatching and charging infrastructure configuration and flexible capacity design for transit services.

2.1. Integrated Optimization of Vehicle Dispatching and Charging Infrastructure Configuration

Recently, the EB transport planning process has become increasingly important as the electrification of urban public transport continues to advance [9–13]. Integrated planning for multi-problems increases the complexity and difficulty of solving the problem exponentially, compared with the step-by-step planning for a single problem. However, integrated planning can not only further decrease the transit system's operational costs, but also enhance the transit service's efficiency [14]. Hence, more and more researchers focus on the integrated optimization of two or more problems in the EB transport planning process, for instance, the integration of vehicle dispatching and charging infrastructure configuration [15,16]. Among them, charging infrastructure configuration includes the charging

station location, number of chargers, battery capacity equipped in vehicles, etc. [17,18] Targeting the minimization of the overall operating costs, Wang et al. [19] and Hu et al. [20] collaboratively optimized the EB charging plan, number of chargers, and charging station location. Liu et al. [21] presented a collaborative optimization model for finding the optimal EB charging station location, number of chargers, charger power, and EB charging plan aimed at minimizing the costs of passengers' waiting time and the EB system's operating costs. McCabe et al. [22] presented an approach to concurrently determine the EB charger location, EB charging plan, and number of chargers by optimizing the tradeoff between the investment costs of charging facilities and operational performance. Aiming at minimizing total operational costs, He et al. [8] formulated a joint optimization model to determine the EB dispatching plan, EB charging plan, and charging infrastructure planning.

In addition, infrastructure configuration schemes interact with each other [23,24]. For instance, the number of chargers and the charging station location affect the EB charging plan, thus influencing the fleet size [25,26]. Aiming at minimizing the overall implementation costs, Ke et al. [27] established a model to find the optimal EB fleet size, number of chargers, and battery capacity. Liu et al. [28] formulated an optimal model to simultaneously determine the battery capacity and fast-charging station deployment plan under energy consumption uncertainty. He et al. [29] developed an EB fast-charging station deployment approach aimed at minimizing the electricity demand charges, battery acquisition costs, energy storage systems construction costs, and fast-charging stations construction costs. Alwesabi et al. [30] formulated a joint optimization model to concurrently determine the battery capacity and dynamic wireless charging facilities' location. Considering integrated photovoltaic and energy storage systems, Liu et al. [31] presented a charging station planning model aimed at minimizing the charging infrastructure construction costs, charging costs, EB acquisition costs, and carbon emission costs.

2.2. Flexible Capacity Design for Transit Services

AMBs can be physically coupled or uncoupled as operationally required, thus enabling the provision of transit services with flexible capacity [3,32–35]. Chen et al. [36] and Chen et al. [37] determined the optimal departure frequency of AMBs and vehicle capacity under oversaturated traffic by employing discrete modeling and continuous modeling approaches, respectively. Shi et al. [38] concentrated on the collaborative optimization of the departure frequency and the length of AMB for each trip for shared corridors to minimize operating costs and passengers' waiting time. Considering time-dependent travel demand, Ji et al. [6] presented a bi-objective (minimizing passengers' waiting time and total empty seats of AMBs) optimization model to simultaneously determine the timetable, vehicle formation, and AMB dispatching plan. Aiming at minimizing the travel time costs of passengers and operational costs, Pei et al. [39] formulated a joint model to find the optimal vehicle capacity and headway in a modular transit network system (MTNS). Tian et al. [40] formulated a collaborative optimization model to concurrently determine the intermediate special stations' location and capacity in an MTNS. Considering temporal dependencies on passenger demand and limited availability of the AMBs at stations, Tian et al. [41] established an AMB dispatching and vehicle formation integrated optimization model to minimize passengers' waiting time costs, bus companies' operating costs, and re-balancing costs of the AMBs. Khan et al. [4] designed a stop-skipping strategy leveraging physical coupling and uncoupling features of AMBs to minimize the passengers' travel time. Aiming at minimizing the AMB system's overall operating costs, Liu et al. [7] established a collaborative optimization model to find the optimal timetable, AMB dispatching plan, and vehicle formation. This model permitted the AMB to uncouple from one vehicle and couple to another vehicle in either direction on a bi-directional route. Guo et al. [42] applied AMBs to customized on-demand bus services and designed a two-phase method to determine the optimal AMB routing plan and charging plan.

The aforementioned studies have offered some suggestions for the operation and planning strategy of AMBs. However, the charging scheduling of AMBs was not considered

in the aforementioned studies. There are significant differences in the development of a charging plan between AMBs and conventional electric buses. Investigating the charging scheduling of AMBs is imperative. Therefore, this paper proposes a collaborative optimization method for concurrently determining the AMB dispatching plan, charging plan, fleet size, number of chargers, and battery capacity, with the goal of minimizing operating costs.

3. Methodology

3.1. Problem Description

In this study, one trip refers to the process of an AMB departing from the upbound departure station of a route to the upbound terminal station (i.e., the outbound departure station) and back to the upbound departure station (i.e., the outbound terminal station). Let i ($i = 1, 2, \dots, I$) represent the trip number on the route, where I is the total number of trips scheduled to operate every day. Let U represent the total number of AMBs deployed on the route and u ($u = 1, 2, \dots, U$) denote the AMB number. Let B denote the battery capacity configured on AMBs. The charging station for AMBs is located at the upbound departure station on the route and is constructed with R chargers. Let r ($r = 1, 2, \dots, R$) denote the charger number. It is worth noting that a trip can be performed by multiple AMBs. We assume the energy is provided by the first AMB when multiple AMBs are coupled together to serve a trip. Figure 1 gives an example of three AMBs coupling together to serve a trip.

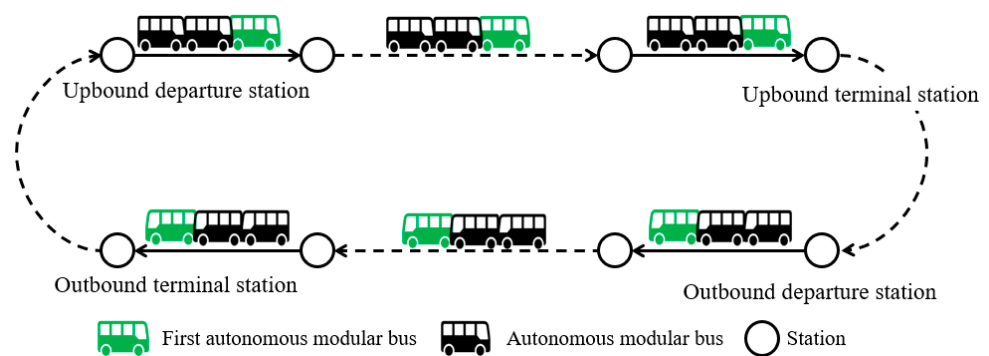


Figure 1. Schematic diagram of multiple AMBs performing a trip together.

The 0–1 variables x_i^u and y_i^u are used to represent the relationship between AMB u and trip i . If AMB u serves trip n and AMB u is the first vehicle, then $x_i^u = 1$ and $y_i^u = 0$; if AMB u serves trip n and AMB u is not the first vehicle, then $x_i^u = 0$ and $y_i^u = 1$; otherwise, $x_i^u = y_i^u = 0$. If AMB u serves trip j after completing trip i , then $h_{i,j}^u = 1$; otherwise, $h_{i,j}^u = 0$. Furthermore, if the first trip AMB u needs to perform is trip j , then $h_{0,j}^u = 1$; otherwise, $h_{0,j}^u = 0$.

The 0–1 variable d_i^u is used to indicate whether AMB u is charged after serving trip i . If AMB u charges after serving trip i , then $d_i^u = 1$; otherwise, $d_i^u = 0$. Here we discretize time domain into consecutive time steps $k \in \{1, 2, \dots, K\}$. The following 0–1 variables are introduced to obtain the charging start time and end time of AMB. If AMB u starts charging in time step k after serving trip i , then $d_{i,k}^{u,start} = 1$; otherwise, $d_{i,k}^{u,start} = 0$. If AMB u ends charging in time step k after serving trip i , then $d_{i,k}^{u,end} = 1$; otherwise, $d_{i,k}^{u,end} = 0$. If AMB u is charged in time step k after serving trip i , then $d_{i,k}^u = 1$; otherwise, $d_{i,k}^u = 0$.

3.2. Battery State of Charge of Autonomous Modular Bus Calculation

The AMB starts operation with a battery SOC of SOC_{max} . The battery SOC is always within the interval $[SOC_{min}, SOC_{max}]$ during operation [43]. The calculation of battery SOC of AMB u at the beginning of the trip j (SOC_j^u) can be discussed in the following three conditions, under the mode that the first vehicle of the coupled AMBs provides energy during the entire trip.

Case 1: The first trip AMB u needs to perform is trip j , i.e., $h_{0,j}^u = 1$. Under this condition, SOC_j^u can be calculated as follows:

$$\text{SOC}_j^u = \text{SOC}_{\max}, \quad h_{0,j}^u = 1 \quad (1)$$

Case 2: AMB u performs trip j after completing trip i and AMB u is the first vehicle when serving trip i , i.e., $x_i^u = 1$ and $h_{i,j}^u = 1$. Under this condition, SOC_j^u can be calculated as follows:

$$\text{SOC}_j^u = \text{SOC}_i^u - \frac{W_i}{B} \times 100\%, \quad x_i^u = 1 \text{ and } h_{i,j}^u = 1 \quad (2)$$

where W_i is the energy consumption of trip i , kWh; SOC_i^u is battery SOC of AMB u at the beginning of the trip i , %.

W_i is expressed as follows [44]:

$$\ln W_i = -8.3743 + 0.5523 \ln L + 0.7814 \ln M_i + 0.3543 \ln T_i + 0.0077 |\bar{\zeta}_i - 23.7| \quad (3)$$

where L denotes the distance of one trip, km; M_i represents the total weight of the vehicle on trip i , kg; T_i is trip i 's travel time, min; $\bar{\zeta}_i$ is the average ambient temperature during operation of trip i , °C.

For the AMB dispatching problem in this study, the calculation of M_i is as follows:

$$M_i = \tau_i M_{pas} + \sum_{i=1}^I (x_i^u + y_i^u) (M_{bus} + M_B) \quad (4)$$

$$M_B = 1000(B/\eta) \quad (5)$$

where τ_i is trip i 's average number of passengers, pax; M_{pas} is the average passenger mass, kg; M_{bus} is the weight of an AMB (without battery), kg; M_B is the weight of one battery, kg; η is battery energy density, Wh/kg.

Case 3: AMB u performs trip j after completing trip i and AMB u is not the first vehicle when serving trip i , i.e., $y_i^u = 1$ and $h_{i,j}^u = 1$. Under this condition, SOC_j^u can be calculated as follows:

$$\text{SOC}_j^u = \text{SOC}_i^u, \quad y_i^u = 1 \text{ and } h_{i,j}^u = 1 \quad (6)$$

3.3. Objective Function Formulation

The objective of the collaborative optimization model formulated in this paper is to minimize the operational costs, including the charger deployment costs Z_1 , AMB body (without battery) acquisition costs Z_2 , battery acquisition costs Z_3 , and charging costs Z_4 .

(1) Charger deployment costs calculation

The charger deployment costs are determined by the average daily acquisition costs of a charger c_{pile} (CNY) and the number of chargers. The calculation method of charger deployment costs Z_1 is as follows:

$$Z_1 = c_{pile}R \quad (7)$$

(2) AMB body acquisition costs calculation

The AMB body acquisition costs are determined by the average daily acquisition costs of an AMB body c_{AMB} (CNY) and the number of AMBs on the route. The AMB body acquisition costs Z_2 can be calculated as follows:

$$Z_2 = c_{AMB}U \quad (8)$$

(3) Battery acquisition costs calculation

Battery acquisition costs are determined by the average daily costs of acquisition per kWh of battery c_{battery} (CNY), battery capacity, and the number of AMBs. The calculation of battery acquisition costs Z_3 is as follows:

$$Z_3 = c_{\text{battery}}UB \quad (9)$$

(4) Charging costs calculation

The charging costs of AMBs are determined by charging times and time-of-use tariff. The calculation method of charging costs Z_4 is

$$Z_4 = \sum_{u=1}^U \sum_{i=1}^I \sum_{k=1}^K \frac{d_{i,k}^u c_k P}{60} \quad (10)$$

where c_k is the electricity price of time step k , CNY/kWh; P is charger power, kW.

3.4. Model Formulation

Aiming at minimizing the operation costs, a collaborative optimization model is established using battery capacity (B), AMB fleet size (U), number of chargers (R), AMB dispatching plan (x_i^u , y_i^u , and $h_{i,j}^u$), and AMB charging plan (d_i^u and $d_{i,k}^u$) as optimization variables. The model is established as follows:

$$\min Z = Z_1 + Z_2 + Z_3 + Z_4 \quad (11)$$

$$\text{s.t. } \sum_{u=1}^U x_i^u = 1, \quad \forall i \quad (12)$$

$$\sum_{u=1}^U n_{\text{bus}}(x_i^u + y_i^u) \geq N_i^{\text{req}}, \quad \forall i \quad (13)$$

$$h_{i,j}^u \left(t_i^{\text{end}} + \sum_{k=1}^K k (d_{i,k}^u - d_{i,k}^{\text{start}}) - t_j^{\text{start}} \right) \leq 0, \quad \forall u, i, j \quad (14)$$

$$x_i^u \left(\text{SOC}_i^u - \frac{W_i}{B} \times 100\% \right) \geq \text{SOC}_{\min} \quad (15)$$

$$\sum_{k=1}^K d_{i,k}^{\text{start}} = d_i^u, \quad \forall i, u \quad (16)$$

$$\sum_{k=1}^K d_{i,k}^{\text{end}} = d_i^u, \quad \forall i, u \quad (17)$$

$$\sum_{k=1}^K k (d_{i,k}^{\text{end}} - d_{i,k}^{\text{start}}) \leq B \times \left(\text{SOC}_{\max} - \left(\text{SOC}_i^u - \frac{W_i}{B} \times 100\% \right) \right) \times 60/P, \quad \text{if } d_i^u = 1, \forall i \quad (18)$$

$$\sum_{u=1}^U \sum_{i=1}^I d_{i,k}^u \leq R, \quad \forall k \quad (19)$$

$$x_i^u, y_i^u, h_{i,j}^u, d_i^u \in \{0, 1\} \quad (20)$$

$$x_i^u + y_i^u = 1, \quad \text{if } h_{i,j}^u = 1 \quad (21)$$

$$x_j^u + y_j^u = 1, \quad \text{if } h_{i,j}^u = 1 \quad (22)$$

$$B_{\min} \leq B \leq B_{\max} \quad (23)$$

$$B, R, U \in \mathbb{N}^+ \quad (24)$$

where n_{bus} is the rated passenger load of an AMB, pax ; N_i^{req} is the maximum number of cross-sectional passengers for trip i , pax ; t_i^{end} is trip i 's ending time; t_j^{start} is trip j 's starting time; B_{min} and B_{max} are the allowable minimum and maximum battery capacity for AMBs, respectively, kWh.

Equation (12) indicates that each trip has exactly one AMB to provide energy. Equation (13) ensures that the boarding demand of passengers is satisfied for each trip. Equation (14) represents the time feasibility constraint that ensures AMB u is able to perform trip j on time after finishing trip i . Equation (15) is the power constraint that ensures the battery's SOC of AMB u remains greater than SOC_{min} after finishing trip i . Equation (16) expresses that if AMB u is charged after completing trip i , it must start charging at a certain time step k . Equation (17) implies that if AMB u is charged after completing trip i , it must end charging at a certain time step k . Equation (18) depicts the maximum charging time constraint of AMB, ensuring that the battery's SOC of AMB can never exceed SOC_{max} . Equation (19) ensures the number of AMBs in charging cannot be greater the number of chargers at any time. Equations (20)–(24) present the optimization variables' value constraints.

3.5. Solution Algorithm

A nonlinear mixed-integer programming model with a large number of dimensions is developed in this paper. The PSO algorithm exhibits a fast convergence speed when solving nonlinear and multi-dimensional optimization problems. However, PSO easily converges prematurely and falls into the local optimal solution, leading to slow convergence at a later stage. Introducing CA into PSO can increase the population diversity and overcome the problem of being trapped in the local optimal solution during the multi-peak optimization process, and can thus obtain the global optimal solution.

In addition, feasible schemes for charging infrastructure configuration are relatively limited compared to feasible AMB dispatching plans and charging plans. Accordingly, we use a combination of enumeration, CA, and PSO for designing a hybrid intelligent algorithm to address the developed model. Specifically, we first use the enumeration method to provide feasible charging infrastructure configuration schemes for battery capacity, AMB fleet size, and number of chargers. Then, the hybrid intelligent algorithm combining CA and PSO is employed to solve the optimal AMB dispatching plan and charging plan for each feasible charging infrastructure configuration scheme, and obtain the bus route's operating costs. Finally, the bus route's operating costs for the feasible schemes are compared and the minimum costs charging infrastructure configuration plan, AMB dispatching plan, and charging plan are output.

The hybrid intelligent algorithm is designed with the following specific steps.

Step 1: Determine the feasible charging infrastructure configuration plans by enumeration, including the feasible fleet size U_{fea} ($U_{\text{fea}} = U_{\text{fea, min}}, U_{\text{fea, min}} + 1, \dots, U_{\text{fea, max}} - 1, U_{\text{fea, max}}$), number of chargers R_{fea} ($R_{\text{fea}} = R_{\text{fea, min}}, R_{\text{fea, min}} + 1, \dots, R_{\text{fea, max}} - 1, R_{\text{fea, max}}$), and battery capacity $B_{\text{fea}}^{R_{\text{fea}}}$ ($B_{\text{fea}}^{R_{\text{fea}}} = B_{\text{fea, min}}^{R_{\text{fea}}}, B_{\text{fea, min}}^{R_{\text{fea}}} + 1, \dots, B_{\text{fea, max}}^{R_{\text{fea}}} - 1, B_{\text{fea, max}}^{R_{\text{fea}}}$).

Step 2: Solve the AMB dispatching plan and charging plan using a hybrid intelligent algorithm combining CA and PSO for each charging infrastructure configuration plan under the combination of U_{fea} , R_{fea} , and $B_{\text{fea}}^{R_{\text{fea}}}$.

Step 2.1: Set the number of iterations to $s = 0$. Let the maximum number of iterations to S and the population size to E .

Step 2.2: Generate the initial population. The population contains E particles generated randomly in the parameter space. Each particle has two attributes: velocity and position.

The optimization variables x_i^u , y_i^u , and d_i^u are all 0–1 matrices of $I \times U$. Therefore, the search space $G = 3I \times U$. The velocity space and position space of the particle swarm are both matrices of $S \times G$. As a dependent variable, the value of $h_{i,j}^u$ can be obtained implicitly by optimizing the aforementioned variables.

Step 2.3: Calculate the affinity θ_e of particle e . The calculation method is as follows:

$$\theta_e = 1/(Z_{e,1} + Z_{e,2} + Z_{e,3} + Z_{e,4}) \quad (25)$$

where $Z_{e,1}$, $Z_{e,2}$, $Z_{e,3}$, and $Z_{e,4}$ are the charger deployment costs, AMB body acquisition costs, battery acquisition costs, and charging costs for the feasible solution represented by particle e , respectively, CNY.

Step 2.4: Update the optimal position $F_{e,\text{best}}$ searched by particle e up to now and the optimal position $F_{\text{best,all}}$ searched by the whole particle swarm until now.

Step 2.5: Determine whether $s \geq S$. If yes, proceed to Step 2.11; otherwise, proceed to Step 2.6.

Step 2.6: Update the velocity and position of all particles based on Equations (26) and (27). And restrict the velocity not to exceed the boundary $[-V_{\text{max}}, V_{\text{max}}]$

$$v_{e,g}(s+1) = \omega v_{e,g}(s) + c_1 r_1 (F_{e,\text{best}} - f_{e,g}(s)) + c_2 r_2 (F_{\text{best,all}} - f_{e,g}(s)) \quad (26)$$

$$f_{e,g}(s+1) = f_{e,g}(s) + v_{e,g}(s+1) \quad (27)$$

where $v_{e,g}(s+1)$ and $f_{e,g}(s+1)$ are the velocity and position in the g -th dimension of the $s+1$ -st generation particle e , respectively; c_1 and c_2 represent acceleration constants; ω denotes the inertia weight; r_1 and r_2 are random numbers between $[0, 1]$.

Step 2.7: Select τ particles with high affinity and write them to the set A_m . The remaining $E - \tau$ particles are written to the set A_r .

Step 2.8: Cloning. Sort the particles by affinity from highest to lowest and select ζ particles with the highest affinity in A_m to clone. The higher the affinity, the more particles will be cloned.

Step 2.9: Mutation. Sort the cloned particles according to the affinity from high to low. The mutation rate becomes smaller with the increase in affinity.

Step 2.10: Recalculate the affinity of each particle after mutation according to Equation (25). Select τ particles with high affinity to write into the set A_m , and return to Step 2.3.

Step 2.11: Export the optimal AMB dispatching plan and charging plan under the charging infrastructure configuration plan of U_{fea} , R_{fea} , and $B_{\text{fea}}^{R_{\text{fea}}}$.

Step 3: Compare the route operating costs of all feasible schemes.

Step 4: Output the minimum operating costs scheme, i.e., the optimal AMB dispatching plan, charging plan, and charging infrastructure configuration plan.

4. Case Study

4.1. Data Investigation

In this subsection, an actual electric bus route in a specific city in China was adopted as the research object and the data from 14 March 2023 were utilized to validate the established method. The route consists of 19 stations, as illustrated in Figure 2. Chargers were deployed in Terminal I. As described in Section 2.1, the process of the AMB running from Terminal I to Terminal II and returning to Terminal I is one trip. The operating mileage of one trip is 17.3 km. The departure time of the first and last trips of the route is 5:30 and 20:30, respectively. The operating time is divided into nine operating periods and the specific operational information of each period is listed in Table 1. The city implements a time-of-use tariff policy, and the related information is presented in Table 2. Table 3 gives the average temperatures for each hour during operation.

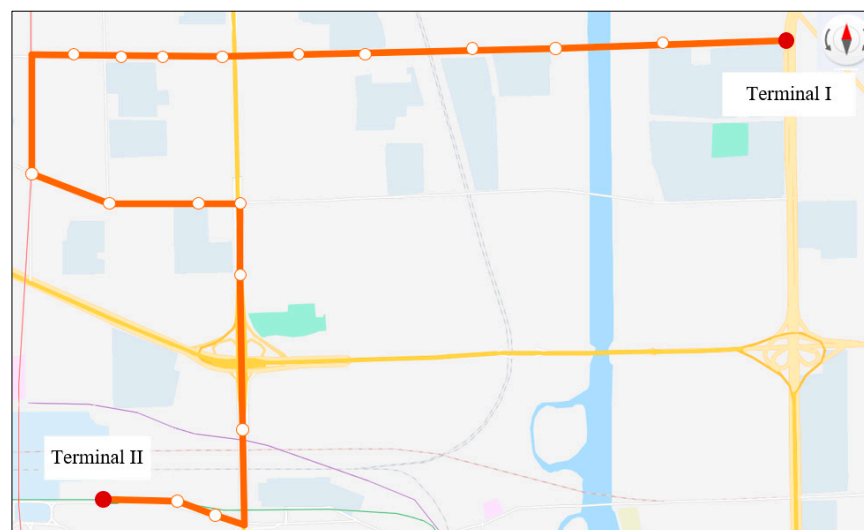


Figure 2. Layout of the real route.

Table 1. The specific operational information of each period.

Index	Time Period	Headway (min)	Number of Trips	Travel Time (min)
1	5:30–6:30	6	10	53
2	6:30–8:30	5	24	58
3	8:30–10:00	6	15	55
4	10:00–15:00	8	38	53
5	15:00–16:00	6	10	58
6	16:00–17:30	5	18	63
7	17:30–18:30	6	10	58
8	18:30–19:30	8	8	53
9	19:30–20:30	10	7	50

Table 2. Time-of-use tariff schedule.

Index	Time Period	Electricity Price (CNY/kWh)
1	6:00–9:00	1.0866
2	9:00–11:30	1.3574
3	11:30–15:30	1.0866
4	15:30–21:00	1.3574
5	21:00–23:00	1.0866
6	23:00–6:00	0.8158

Table 3. Average temperatures for each hour during operation.

Index	Time Period	Average Temperature (°C)	Index	Time Period	Average Temperature (°C)
1	05:00–06:00	−3	9	14:00–15:00	3
2	06:00–07:00	−3	10	15:00–16:00	2
3	07:00–08:00	−2	11	16:00–17:00	1
4	08:00–09:00	0	12	17:00–18:00	0
5	09:00–10:00	1	13	18:00–19:00	−2
6	10:00–11:00	2	14	19:00–20:00	−3
7	11:00–12:00	2	15	20:00–21:00	−4
8	13:00–14:00	3			

The maximum number of cross-sectional passengers on each trip is listed in Appendix A. Referring to the actual condition, we assume that the AMBs are equipped with LiFePO₄

batteries. The battery system energy density (η) is 140.13 Wh/kg. In actual operation, the rated passenger load for an electric bus on the route is 77, the mass of the bare vehicle (without battery) is 9190 kg, and the purchase costs (without battery) are 522,490 CNY. The rated passenger load for an AMB is 10 [5], thus assuming that the bare mass of an AMB (without battery) is 1193.5 kg ($10/77 \times 9190$ kg), and the purchase costs (without battery) are 67,855.8 CNY ($10/77 \times 522,490$ CNY). The average daily acquisition costs of the infrastructure can be obtained by dividing the acquisition costs by the useful life. The charger acquisition costs are 100,000 CNY and the acquisition costs of the battery are 1400 CNY per kWh. The charger can be used for 10 years. The battery's useful life is 6 years [29]. Table 4 shows the values of other parameters in the developed model.

Table 4. Values of some parameters of the developed model.

Parameter	Value	Parameter	Value
c_{pile}	27.4 CNY	SOC _{min}	20%
c_{AMB}	30.98 CNY	SOC _{max}	95%
$c_{battery}$	0.639 CNY	B_{min}	10 kWh
P	120 kW	B_{max}	60 kWh
M_{pas}	60 kg		

4.2. Optimization Results and Analysis

We used Python 3.8.2 to address the formulated model. For the optimal solution obtained, the route operating costs $Z = 4794.302$ CNY, the AMB fleet size $U = 98$, the battery capacity $B = 16$ kWh, and the number of chargers $R = 1$. Among them, the charger deployment costs are 27.4 CNY, AMB body acquisition costs are 3036.04 CNY, battery acquisition costs are 1001.952 CNY, and charging costs are 728.91 CNY. It can be seen that the AMB body acquisition costs are the largest expenditure in the route operation, constituting 63.33% of the total operating costs. The charger deployment costs, battery acquisition costs, and charging costs account for 0.57%, 20.90%, and 15.20% of the overall route operating costs, respectively. The charging of AMBs all takes place at night after the end of operation. The AMB dispatching plan is displayed in Table 5.

Table 5. AMB dispatching plan.

Trip No.	AMB No.	W_i (kWh)	Trip No.	AMB No.	W_i (kWh)
1	1-2-3-4-5-6	7.13	71	96-67-28-36	5.01
2	7-8-24-10-11-12-13	8.08	72	21-18-19-20	5.08
3	15-14-16	4.22	73	32-33-34-30-31	5.86
4	74-18-19-20-21-22-23	8.08	74	17-60-57-58-59-73	6.86
5	9-25-26-27	5.19	75	65-66-25-63-64-29	6.84
6	28-29-30-31-32-33-34-35	9.03	76	26-43-70-71-83-69-48	7.68
7	36-37-38-39	5.11	77	56-61-55	3.97
8	40-41-42-43	5.28	78	15-52-53-54-14	5.97
9	44-45-46	4.14	79	11-12-9	4.03
10	47-48-1-2-3-4-5-6	8.95	80	10-84-40-47	4.93
11	49-7-8-9-10-11-12-13	9.32	81	68-37-38-39	4.95
12	50-51-52-53-54-14-15-16	9.29	82	3-2-35	3.91
13	55-56-57-58-59-60-61	8.41	83	45-46-81-82	4.91
14	62-17-18-19-20-21-22-23	9.25	84	79-80-78	3.99
15	63-64-65-66-24-25-26-27	9.24	85	76-77-75-16-50	5.88
16	29-30-31-32-33-34	7.45	86	90-86-87-88-89	5.86
17	35-67-28-36-37-38-39-68	9.20	87	95-91-92-93-94	5.85
18	41-40-69-42-43-70-71	8.26	88	42-27-22-23-51	6.10
19	72-73-74-75-76-77	7.34	89	85-1-41-72	5.25
20	78-79-80-81-82-44-45-46	9.23	90	22-62-17	4.13
21	4-5-6	4.30	91	20-21-18-19	5.13

Table 5. Cont.

Trip No.	AMB No.	W_i (kWh)	Trip No.	AMB No.	W_i (kWh)
22	48-83-84-47-85-1-2-3	9.15	92	39-68-37-38	5.09
23	13-49-7-8-9-10-11-12	9.22	93	65-29-44-64	5.11
24	16-50-51-52-53-54-14-15	9.23	94	5-49-7-6-4	6.17
25	61-55-56-57-58-59-60	8.31	95	31-66-25-63	5.15
26	22-62-17-18-19-20-21	8.38	96	58-59-73-74-60-57	7.20
27	25-63-64-65-66-24	7.38	97	53-54-14-15-52	6.16
28	30-31-32-33-34	6.39	98	64-29-26-63	5.37
29	67-28-36-37-38-39-68	8.10	99	69-48-3-2-35	6.37
30	71-83-69-42-43-70	7.30	100	82-45-46-81-11-12-9	8.38
31	75-76-77	4.07	101	89-90-86-41-72-65-30	8.34
32	74-73	3.10	102	10-84-40-47	5.27
33	81-82-44-45-46	6.20	103	32-33-34	4.31
34	40-84-47-85-1	6.23	104	94-95-91-85-1-56-61-55	9.22
35	9-10-11-12	5.21	105	19-20-21-18-79-80-78	8.40
36	80-78-79	4.14	106	23-25-27-22-51-22-62-17	9.29
37	51-52-53-54-14-15	7.04	107	38-39-68-37-56-61	7.33
38	22-23-25-27	5.12	108	97-96-67-28-36-55-8	8.34
39	57-58-59-60	5.13	109	98-42-43-70-71-83-76	8.36
40	34-30-31-32-33	6.14	110	59-45-74-60-57-58-77-50	9.31
41	18-19-20-21	5.02	111	54-46-15-52-53-16	7.52
42	37-38-39-68	5.19	112	4-5-49-7-6	6.51
43	70-71-83-69-42-43	7.04	113	87-31-66-26-63-81	7.39
44	66-25-63-64-65-29	7.00	114	88-69-48-3-2-35	7.53
45	46-81-82-44-45	6.03	115	92-64-29-10-63-82	7.40
46	6-4-5	4.12	116	93-45-46-81-11-12-33	8.15
47	8-13-49-7	5.19	117	73-89-90-86-41-72-65-30	9.09
48	2-3-35-41-72	6.03	118	14-19-20-21-18-79-80-78	9.08
49	96-67-28-36	5.02	119	75-11-12-9-32-84	7.17
50	12-9-10-11	4.92	120	44-40-47-61-55	6.33
51	17-61-55	4.02	121	24-94-95-91-85-1-56	8.26
52	33-34-30-31-32	5.96	122	83-34-42-43-70-71-23	8.38
53	37-38-39	4.06	123	85-27-22-51-22	6.44
54	52-53-54-14-15	5.93	124	54-62	3.08
55	84-40-47-85-1	5.98	125	88-68-37	4.32
56	27-22-23-26-51	5.94	126	38-56	3.03
57	60-57-58-59-73-74	6.82	127	76-97-96-67-28	6.11
58	43-70-71-83-69-42-48	7.76	128	98-36	2.85
59	45-46-81-82-44	6.03	129	92-61	3.03
60	77-75-76-16-50	5.89	130	64-36-55-8-61	6.25
61	64-66-25-63-65-29	6.89	131	18-4-5-49-7	6.16
62	56-2-35-41-72	5.94	132	69-6-46-15	5.17
62	21-18-19-20	4.97	133	77-57-58	4.10
64	86-87-88-89-90	5.98	134	95-52-53-16	5.17
65	91-92-93-94-95	5.96	135	25-46-81	4.01
66	79-80-78-22-62-17	6.82	136	3-29-10-63-82-45-11	7.90
67	68-37-38-39	5.05	137	90-86-41-72-65	6.10
68	11-12-9-10	5.08	138	39-21-79	4.12
69	6-4-5-49-7	5.96	139	65-44-40	4.02
70	56-61-55-8-13	5.93	140	20-88-68-37	5.21

The suboptimal solution is used to compare with the above optimal solution in this paper. In the suboptimal solution, the route operating costs $Z = 4810.822$ CNY, the AMB fleet size $U = 98$, the battery capacity $B = 16$ kWh, and the number of chargers $R = 2$. Among them, the charger deployment costs are 54.8 CNY, AMB body acquisition costs are 3036.04 CNY, battery acquisition costs are 1001.952 CNY, and charging costs are 718.03 CNY. Compared with the suboptimal solution, the charging costs of the optimal solution are increased by 10.88 CNY. This is because the charging of AMBs occurs in both the nighttime

tariff shoulder period and off-peak period, i.e., 21:00–23:00 and 23:00–6:00. While in the suboptimal solution, the charging of AMBs only occurs in the nighttime tariff off-peak period, i.e., 23:00–6:00. However, the optimal solution reduces the charger deployment costs by 27.4 CNY. Hence, we chose to deploy one charger in the charging station.

We compare the vehicle dispatching plan, charging plan, and charging infrastructure configuration between the proposed method (Plan A) and the current plan using EBs for route operation (Plan B) to verify the effectiveness of the method proposed in this paper.

Plan A: Use AMBs to serve the given trips.

Plan B: Use EBs to serve the given trips. The mass and the purchase costs of the bare EB (without battery) are 9190 kg and 522,490 CNY, respectively. The capacity of an EB is 77 passengers.

As can be seen in Table 6, the route operating costs in Plan A are reduced by 5.92%, equivalent to 301.77 CNY, compared to Plan B. It is apparent that the major reason for the reduction in the route operating costs in Plan A is the significant decrease in the charging costs. This is due to the significant reduction in the route operating energy consumption in Plan A compared to Plan B. The daily route operating energy consumption in Plan B is 1155.79 kWh, whereas the daily route operating energy consumption in Plan A is only 880.16 kWh. Compared to Plan B, the daily route operating energy consumption in Plan A is reduced by 23.85%, approximately equal to 275.63 kWh. Figure 3 illustrates the operational energy consumption for each trip. It is observed that the trip energy consumption of Plan A in the off-peak hours is much lower than that of Plan B. This is because Plan A is able to flexibly adjust the number of vehicles to perform a trip according to passenger demand. During low passenger demand periods, fewer AMBs are needed to complete a trip, vehicle weight is reduced, and thus, trip energy consumption is reduced.

Table 6. Comparison of results under two plans.

Plan	Plan A	Plan B
U	98	13
B (kWh)	16	120
R	1	2
Z (CNY)	4794.302	5096.07
Z_1 (CNY)	27.4	54.8
Z_2 (CNY)	3036.04	3101.54
Z_3 (CNY)	1001.952	996.84
Z_4 (CNY)	728.91	942.89

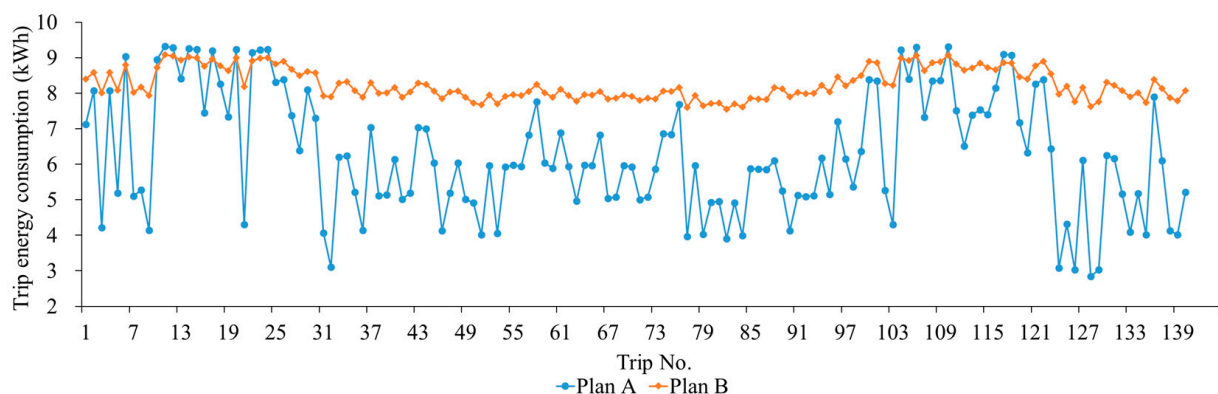


Figure 3. Trip energy consumption.

Similarly, as Plan A can flexibly adjust the vehicle capacity of each trip according to passenger demand, the utilization of vehicles in Plan A also increases, especially during off-peak hours. Figure 4 depicts the utilization of vehicles for each trip.

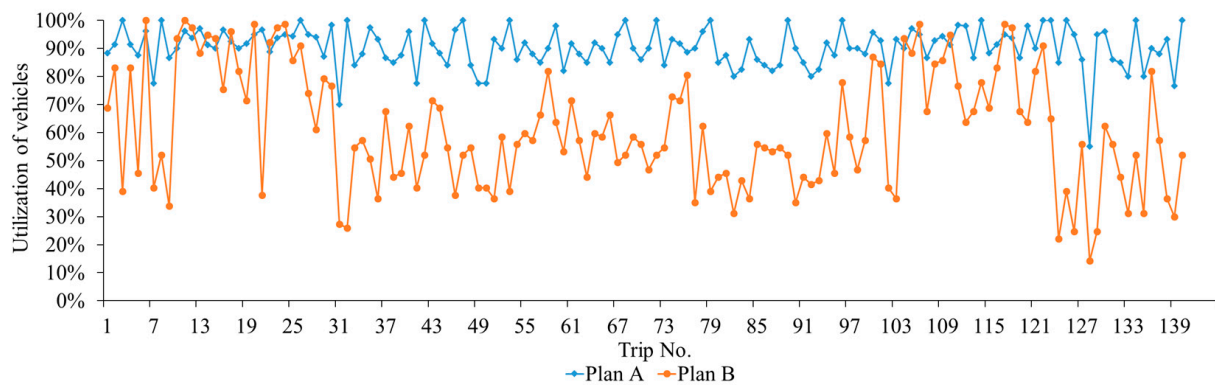


Figure 4. Utilization of vehicles.

Moreover, we find that the trip energy consumption in Plan A is likely to be higher than that in Plan B, and utilization of vehicles may be lower than that in Plan B during peak hours. This is because the rated passenger load of a vehicle in historical operations is 77, i.e., the maximum historical passenger demand for one trip is 77 passengers, whereas the rated passenger load of an AMB is 10. Plan A will equip eight AMBs for one trip when passenger demand is in the range of [71, 77] during peak hours. In this case, the vehicle weight and vehicle capacity for one trip in Plan A are larger than in Plan B, resulting in higher trip energy consumption and lower utilization of vehicles.

5. Conclusions

The emergence of AMBs is of great significance in enhancing the sustainability of the urban public transportation system. This study develops a collaborative optimization method for bus route operating AMBs to concurrently determine the AMB dispatching plan, charging scheduling plan, and charging infrastructure configuration scheme, under the circumstance that the first vehicle of the coupled AMBs provides energy during the entire trip. A hybrid intelligent algorithm was designed to resolve the established model. Numerical experiments were carried out utilizing the data of an actual EB route. The findings are as follows:

- (i) The collaborative optimization method developed in this paper can flexibly adjust the number of vehicles to perform a trip according to passenger demand, leading to lower vehicle weight during off-peak hours. It realizes decreased trip energy consumption, improved vehicle utilization, and reduced route operating costs.
- (ii) Utilizing AMB for bus routes can effectively reduce daily operating costs and operational energy consumption, compared to using conventional EB. The former can be reduced by 5.92%, approximately 301.77 CNY. The latter can be reduced by 23.85%, approximately equal to 275.63 kWh.

However, there are some limitations to this study. We neglected the impact of ambient temperature on people's choice of public transport traveling mode [45]. The coupling and decoupling operations of AMBs at any stops were not considered. Future work is required to further discuss the above issues to address the spatial fluctuations in passenger demand, which can further promote the realization of a sustainable urban public transportation system. In addition, for future research, the proposed collaborative optimization method can be potentially extended to multiple routes and multiple charging modes (e.g., multiple vehicles of the coupled AMBs providing energy jointly during the trip). An exact efficient solution algorithm will be studied in the future.

Author Contributions: Conceptualization, A.C. and Y.C.; methodology, Y.C. and C.W.; software, Y.B.; validation, A.C., C.W. and Y.B.; investigation, Y.C.; data curation, Y.C.; writing—original draft preparation, A.C. and C.W.; writing—review and editing, Y.B.; visualization, Y.B. All authors have read and agreed to the published version of the manuscript.

Funding: This research was funded by the Youth Science and Technology Innovation and Entrepreneurship Outstanding Talent (Team) Project of Jilin Province, grant number 20230508048RC.

Institutional Review Board Statement: Not applicable.

Informed Consent Statement: Not applicable.

Data Availability Statement: Data will be made available upon reasonable request.

Conflicts of Interest: The authors declare no conflicts of interest.

Appendix A

Table A1. The maximum number of cross-sectional passengers on each trip.

Trip No.	Maximum Number of Cross-Sectional Passengers (Pax)	Trip No.	Maximum Number of Cross-Sectional Passengers (Pax)	Trip No.	Maximum Number of Cross-Sectional Passengers (Pax)
1	53	48	42	95	35
2	64	49	31	96	60
3	30	50	31	97	45
4	64	51	28	98	36
5	35	52	45	99	44
6	77	53	30	100	67
7	31	54	43	101	65
8	40	55	46	102	31
9	26	56	44	103	28
10	72	57	51	104	72
11	77	58	63	105	68
12	75	59	49	106	76
13	68	60	41	107	52
14	73	61	55	108	65
15	72	62	44	109	66
16	58	62	34	110	73
17	74	64	46	111	59
18	63	65	45	112	49
19	55	66	51	113	52
20	76	67	38	114	60
21	29	68	40	115	53
22	71	69	45	116	64
23	75	70	43	117	76
24	76	71	36	118	75
25	66	72	40	119	52
26	70	73	42	120	49
27	57	74	56	121	63
28	47	75	55	122	70
29	61	76	62	123	50
30	59	77	27	124	17
31	21	78	48	125	30
32	20	79	30	126	19
33	42	80	34	127	43
34	44	81	35	128	11
35	39	82	24	129	19
36	28	83	33	130	48
37	52	84	28	131	43
38	34	85	43	132	34
39	35	86	42	133	24
40	48	87	41	134	40
41	31	88	42	135	24
42	40	89	40	136	63
43	55	90	27	137	44

Table A1. Cont.

Trip No.	Maximum Number of Cross-Sectional Passengers (Pax)	Trip No.	Maximum Number of Cross-Sectional Passengers (Pax)	Trip No.	Maximum Number of Cross-Sectional Passengers (Pax)
44	53	91	34	138	28
45	42	92	32	139	23
46	29	93	33	140	40
47	40	94	46		

References

- Liu, Y.; Francis, A.; Hollauer, C.; Lawson, M.C.; Shaikh, O.; Cotsman, A.; Bhardwaj, K.; Banboukian, A.; Li, M.; Webb, A.; et al. Reliability of electric vehicle charging infrastructure: A cross-lingual deep learning approach. *Commun. Transp. Res.* **2023**, *3*, 100095. [\[CrossRef\]](#)
- Ji, J.; Bie, Y.; Shi, H.; Wang, L. Energy-saving speed profile planning for a connected and automated electric bus considering motor characteristic. *J. Clean. Prod.* **2024**, *448*, 141721. [\[CrossRef\]](#)
- Zhang, Z.; Tafreshian, A.; Masoud, N. Modular transit: Using autonomy and modularity to improve performance in public transportation. *Transp. Res. Part E Logist. Transp. Rev.* **2020**, *141*, 102033. [\[CrossRef\]](#)
- Khan, Z.S.; He, W.; Menéndez, M. Application of modular vehicle technology to mitigate bus bunching. *Transp. Res. Part C Emerg. Technol.* **2023**, *146*, 103953. [\[CrossRef\]](#)
- Liu, X.; Qu, X.; Ma, X. Improving flex-route transit services with modular autonomous vehicles. *Transp. Res. Part E Logist. Transp. Rev.* **2021**, *149*, 102331. [\[CrossRef\]](#)
- Ji, Y.; Liu, B.; Shen, Y.; Du, Y. Scheduling strategy for transit routes with modular autonomous vehicles. *Int. J. Transp. Sci. Technol.* **2021**, *10*, 121–135. [\[CrossRef\]](#)
- Liu, Z.; de Almeida Correia, G.H.; Ma, Z.; Li, S.; Ma, X. Integrated optimization of timetable, bus formation, and vehicle scheduling in autonomous modular public transport systems. *Transp. Res. Part C Emerg. Technol.* **2023**, *155*, 104306. [\[CrossRef\]](#)
- He, Y.; Liu, Z.; Song, Z. Joint optimization of electric bus charging infrastructure, vehicle scheduling, and charging management. *Transp. Res. Part D Transp. Environ.* **2023**, *117*, 103653. [\[CrossRef\]](#)
- He, H.; Sun, F.; Wang, Z.; Lin, C.; Zhang, C.; Xiong, R.; Deng, J.; Zhu, X.; Xie, P.; Zhang, S.; et al. China's battery electric vehicles lead the world: Achievements in technology system architecture and technological breakthroughs. *Green Energy Intell. Transp.* **2022**, *1*, 100020. [\[CrossRef\]](#)
- Lin, Y.; Zhang, K.; Shen, Z.J.M.; Ye, B.; Miao, L. Multistage large-scale charging station planning for electric buses considering transportation network and power grid. *Transp. Res. Part C Emerg. Technol.* **2019**, *107*, 423–443. [\[CrossRef\]](#)
- Cong, Y.; Wang, H.; Bie, Y.; Wu, J. Double-battery configuration method for electric bus operation in cold regions. *Transp. Res. Part E Logist. Transp. Rev.* **2023**, *180*, 103362. [\[CrossRef\]](#)
- Qu, X.; Wang, S.; Niemeier, D. On the urban-rural bus transit system with passenger-freight mixed flow. *Commun. Transp. Res.* **2022**, *2*, 100054. [\[CrossRef\]](#)
- Zeng, Z.; Qu, X. What's next for battery-electric bus charging systems. *Commun. Transp. Res.* **2023**, *3*, 100094. [\[CrossRef\]](#)
- Perumal, S.S.; Lusby, R.M.; Larsen, J. Electric bus planning & scheduling: A review of related problems and methodologies. *Eur. J. Oper. Res.* **2022**, *301*, 395–413.
- Chen, G.; Hu, D.; Chien, S.; Guo, L.; Liu, M. Optimizing wireless charging locations for battery electric bus transit with a genetic algorithm. *Sustainability* **2020**, *12*, 8971. [\[CrossRef\]](#)
- He, J.; Yan, N.; Zhang, J.; Yu, Y.; Wang, T. Battery electric buses charging schedule optimization considering time-of-use electricity price. *J. Intell. Connect. Veh.* **2022**, *5*, 138–145. [\[CrossRef\]](#)
- Xylia, M.; Leduc, S.; Patrizio, P.; Silveira, S.; Kraxner, F. Developing a dynamic optimization model for electric bus charging infrastructure. *Transp. Res. Procedia* **2017**, *27*, 776–783. [\[CrossRef\]](#)
- Sang, X.; Yu, X.; Chang, C.T.; Liu, X. Electric bus charging station site selection based on the combined DEMATEL and PROMETHEE-PT framework. *Comput. Ind. Eng.* **2022**, *168*, 108116. [\[CrossRef\]](#)
- Wang, Y.; Huang, Y.; Xu, J.; Barclay, N. Optimal recharging scheduling for urban electric buses: A case study in Davis. *Transp. Res. Part E Logist. Transp. Rev.* **2017**, *100*, 115–132. [\[CrossRef\]](#)
- Hu, H.; Du, B.; Liu, W.; Perez, P. A joint optimisation model for charger locating and electric bus charging scheduling considering opportunity fast charging and uncertainties. *Transp. Res. Part C Emerg. Technol.* **2022**, *141*, 103732. [\[CrossRef\]](#)
- Liu, X.; Qu, X.; Ma, X. Optimizing electric bus charging infrastructure considering power matching and seasonality. *Transp. Res. Part D Transp. Environ.* **2021**, *100*, 103057. [\[CrossRef\]](#)
- McCabe, D.; Ban, X.J. Optimal locations and sizes of layover charging stations for electric buses. *Transp. Res. Part C Emerg. Technol.* **2023**, *152*, 104157. [\[CrossRef\]](#)
- Uslu, T.; Kaya, O. Location and capacity decisions for electric bus charging stations considering waiting times. *Transp. Res. Part D Transp. Environ.* **2021**, *90*, 102645. [\[CrossRef\]](#)

24. Momenitabar, M.; Ebrahimi, Z.D.; Bengtson, K. Optimal placement of battery electric bus charging stations considering energy storage technology: Queuing modeling approach. *Transp. Res. Rec.* **2023**, *2677*, 663–672. [[CrossRef](#)]
25. Das, P.; Kayal, P. An advantageous charging/discharging scheduling of electric vehicles in a PV energy enhanced power distribution grid. *Green Energy Intell. Transp.* **2024**, *3*, 100170. [[CrossRef](#)]
26. Guschinsky, N.; Kovalyov, M.Y.; Rozin, B.; Brauner, N. Fleet and charging infrastructure decisions for fast-charging city electric bus service. *Comput. Oper. Res.* **2021**, *135*, 105449. [[CrossRef](#)]
27. Ke, B.R.; Chung, C.Y.; Chen, Y.C. Minimizing the costs of constructing an all plug-in electric bus transportation system: A case study in Penghu. *Appl. Energy* **2016**, *177*, 649–660. [[CrossRef](#)]
28. Liu, Z.; Song, Z.; He, Y. Planning of fast-charging stations for a battery electric bus system under energy consumption uncertainty. *Transp. Res. Rec.* **2018**, *2672*, 96–107. [[CrossRef](#)]
29. He, Y.; Song, Z.; Liu, Z. Fast-charging station deployment for battery electric bus systems considering electricity demand charges. *Sustain. Cities Soc.* **2019**, *48*, 101530. [[CrossRef](#)]
30. Alwesabi, Y.; Wang, Y.; Avalos, R.; Liu, Z. Electric bus scheduling under single depot dynamic wireless charging infrastructure planning. *Energy* **2020**, *213*, 118855. [[CrossRef](#)]
31. Liu, X.; Liu, X.; Zhang, X.; Zhou, Y.; Chen, J.; Ma, X. Optimal location planning of electric bus charging stations with integrated photovoltaic and energy storage system. *Comput. Aided Civ. Infrastruct. Eng.* **2022**, *38*, 1424–1446. [[CrossRef](#)]
32. Gong, M.; Hu, Y.; Chen, Z.; Li, X. Transfer-based customized modular bus system design with passenger-route assignment optimization. *Transp. Res. Part E Logist. Transp. Rev.* **2021**, *153*, 102422. [[CrossRef](#)]
33. Dakic, I.; Yang, K.; Menendez, M.; Chow, J.Y. On the design of an optimal flexible bus dispatching system with modular bus units: Using the three-dimensional macroscopic fundamental diagram. *Transp. Res. Part B Methodol.* **2021**, *148*, 38–59. [[CrossRef](#)]
34. Wu, J.; Kulcsár, B.; Qu, X. A modular, adaptive, and autonomous transit system (MAATS): An in-motion transfer strategy and performance evaluation in urban grid transit networks. *Transp. Res. Part A Policy Pract.* **2021**, *151*, 81–98. [[CrossRef](#)]
35. Li, Q.; Li, X. Trajectory optimization for autonomous modular vehicle or platooned autonomous vehicle split operations. *Transp. Res. Part E Logist. Transp. Rev.* **2023**, *176*, 103115. [[CrossRef](#)]
36. Chen, Z.; Li, X.; Zhou, X. Operational design for shuttle systems with modular vehicles under oversaturated traffic: Discrete modeling method. *Transp. Res. Part B Methodol.* **2019**, *122*, 1–19. [[CrossRef](#)]
37. Chen, Z.; Li, X.; Zhou, X. Operational design for shuttle systems with modular vehicles under oversaturated traffic: Continuous modeling method. *Transp. Res. Part B Methodol.* **2020**, *132*, 76–100. [[CrossRef](#)]
38. Shi, X.; Chen, Z.; Pei, M.; Li, X. Variable-capacity operations with modular transits for shared-use corridors. *Transp. Res. Rec.* **2020**, *2674*, 230–244. [[CrossRef](#)]
39. Pei, M.; Lin, P.; Du, J.; Li, X.; Chen, Z. Vehicle dispatching in modular transit networks: A mixed-integer nonlinear programming model. *Transp. Res. Part E Logist. Transp. Rev.* **2021**, *147*, 102240. [[CrossRef](#)]
40. Tian, Q.; Lin, Y.H.; Wang, D.Z.; Liu, Y. Planning for modular-vehicle transit service system: Model formulation and solution methods. *Transp. Res. Part C Emerg. Technol.* **2022**, *138*, 103627. [[CrossRef](#)]
41. Tian, Q.; Lin, Y.H.; Wang, D.Z. Joint scheduling and formation design for modular-vehicle transit service with time-dependent demand. *Transp. Res. Part C Emerg. Technol.* **2023**, *147*, 103986. [[CrossRef](#)]
42. Guo, R.; Guan, W.; Vallati, M.; Zhang, W. Modular autonomous electric vehicle scheduling for customized on-demand bus services. *IEEE Trans. Intell. Transp. Syst.* **2023**, *24*, 10055–10066. [[CrossRef](#)]
43. Bie, Y.; Cong, Y.; Yang, M.; Wang, L. Coordinated scheduling of electric buses for multiple routes considering stochastic travel times. *J. Transp. Eng. Part A Syst.* **2023**, *149*, 04023069. [[CrossRef](#)]
44. Ji, J.; Bie, Y.; Zeng, Z.; Wang, L. Trip energy consumption estimation for electric buses. *Commun. Transp. Res.* **2022**, *2*, 100069. [[CrossRef](#)]
45. Li, Z.; Su, S.; Jin, X.; Xia, M.; Chen, Q.; Yamashita, K. Stochastic and distributed optimal energy management of active distribution network with integrated office buildings. *CSEE J. Power Energy Syst.* **2024**, *10*, 504–517.

Disclaimer/Publisher’s Note: The statements, opinions and data contained in all publications are solely those of the individual author(s) and contributor(s) and not of MDPI and/or the editor(s). MDPI and/or the editor(s) disclaim responsibility for any injury to people or property resulting from any ideas, methods, instructions or products referred to in the content.